Available online at www.sciencedirect.com
SCIENCE DIRECT®
Chemical Physics Letters 397 (2004) 289–295
CHEMICAL PHYSICS LETTERS
www.elsevier.com/locate/cplett

Emission and absorption of $Ir(ppy)_2(CO)(Cl)$ – temperature dependence, phosphorescence decay dynamics, and assignment of excited states

W.J. Finkenzeller [a], P. Stößel [b], H. Yersin [a,*]

[a] *Institut für Physikalische und Theoretische Chemie, Universität Regensburg, D-93053 Regensburg, Germany*
[b] *Covion Organic Semiconductors GmbH, Research and Development, D-65926 Frankfurt am Main, Germany*

Received 3 June 2004
Available online 16 September 2004

Abstract

Emission spectra and decay times of $Ir(ppy)_2(CO)(Cl)$ dissolved in THF were recorded for 1.2 K $\leqslant T \leqslant$ 300 K. The emission stems from a triplet state $\mathbf{T_1}$ which is split into three substates by less than 1 cm^{-1}. We classify this state as ^{3}**LC**(ligand centered, ppyππ*) state. At $T = 1.2$ K, the substates emit independently with three individual decay times ($\tau_I = 300$ μs, $\tau_{II} = 85$ μs, $\tau_{III} = 9$ μs) due to slow equilibration processes, i.e. slow spin-lattice-relaxation, between the substates. With increasing temperature, the emission decay becomes monoexponential as a result of fast equilibration. The results are compared to the spectroscopic behavior of $Ir(ppy)_3$ which represents a metal-to-ligand charge transfer ^{3}**MLCT** emitter.

1. Introduction

Recently, Ir(III) compounds have found great attention due to their application in phosphorescent organic light emitting devices (OLEDs) [1–5]. The attractiveness of these materials is related to their high quantum efficiencies of photoluminescence and electroluminescence. $Ir(ppy)_3$ is a prominent example for phosphorescent OLED emitters and has been studied spectroscopically already in early investigations [6,7]. In a recent study [8], we could demonstrate that the lowest triplet is of Ir5d(ppy)π* metal-to-ligand-charge-transfer (MLCT) character. Ab initio calculations [9] come to the same assignment. In this publication, we focus on $Ir(ppy)_2(CO)(Cl)$, since it is of high scientific interest to understand, how the substitution of one ppy ligand affects the photophysics of the compound. It will be shown that the nature of the emitting state is altered. The lowest triplet is assigned as (ppy)ππ* ligand centered (LC) state.

2. Experimental

$Ir(ppy)_2(CO)(Cl)$ was prepared according to the following procedure. A slow stream of carbon monoxide was bubbled through a solution of 1.072 g (1 mmol) of $[Ir(ppy)_2Cl]_2$, which has been synthesized according to [10] in 100 ml of dichloromethane for 5 h. The solution was then reduced in volume to about 10 ml. After addition of 100 ml of *n*-hexane an off-white precipitate formed which was collected on a sintered glass frit and successively washed with five 10 ml portions of *n*-hexane. The raw product was recrystallized from dichloromethane/hexane to yield 1.046 g (92.7%) of pale yellow micro-crystals. Spectroscopic measurements were

* Corresponding author. Fax: +49 941 943 4488.
E-mail address: hartmut.yersin@chemie.uni-regensburg.de (H. Yersin).
URL: http://www.uni-regensburg.de-/~hartmut.yersin.

0009-2614/$ - see front matter © 2004 Elsevier B.V. All rights reserved.
doi:10.1016/j.cplett.2004.08.074

carried out in a solution of $Ir(ppy)_2(CO)(Cl)$ dissolved in tetrahydrofuran (THF) at a concentration of $\approx 10^{-5}$ mol/l.

The optical setup is similar to the one described in [11]. An argon ion laser (Coherent Innova 90) was used as excitation source for cw emission measurements. Investigations at low temperatures were carried out in a He cryostat (Cryovac Kontikryostat IT) in which the helium gas flow and/or heating was controlled. For experiments below 4 K, a bath cryostat was used. Temperature was reduced by pumping off the helium. Emission spectra were corrected for the wavelength dependence of the photomultiplier and monochromator. Decay times were measured using a FAST Comtech (München) multichannel analyzer PC-card. For pulsed excitation, a N_2 laser with $\lambda_{exc} = 337.1$ nm and a pulse duration of 4 ns was applied. For resonant excitation a Lambdaphysik FL2000 Dye laser pumped by a Spectron Sl803 Nd:YAG laser (pulse width 12 ns) was employed. Absorption spectra were recorded with a Varian Cary 300 double-beam spectrometer.

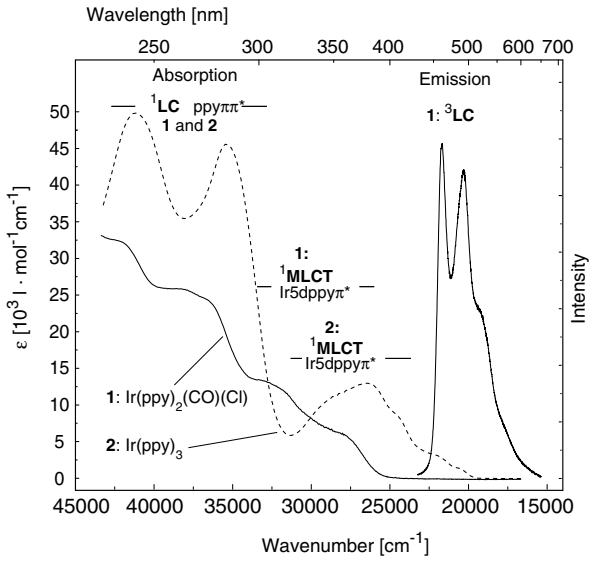

Fig. 1. Absorption and emission spectrum of $Ir(ppy)_2(CO)(Cl)$ (solid line, compound **1**) in THF under ambient conditions. The emission spectrum was measured at a concentration of about 10^{-5} mol/l under cw-excitation at 365 nm. For comparison, the absorption spectrum of $Ir(ppy)_3$ (compound **2**) in THF at ambient temperature is also depicted (dotted line).

3. Results and discussion

3.1. Spectroscopic introduction

In this section, it is intended to present an assignment of the electronic absorption spectrum of $Ir(ppy)_2(CO)(Cl)$. This is strongly facilitated when the spectrum is compared to the one of the already well studied $Ir(ppy)_3$. Fig. 1 reproduces the two absorption spectra of the compounds dissolved in THF and measured under ambient conditions. The classification of the transitions observed for $Ir(ppy)_3$ (compound **2**) is carried out in agreement with literature assignments [6,7,9,12]. In particular, the strong transitions above $\approx 32\,000$ cm^{-1} (312 nm) with maxima at 41 150 cm^{-1} (243 nm, $\epsilon_{max} \approx 505\,00$l/mol cm) and 35 350 cm^{-1} (283 nm, $\epsilon_{max} \approx 455\,00$l/mol cm) are assigned to ligand centered excitations of ppyππ* character. They correspond to singlet ground state $\mathbf{S_0}$ to ^{1}**LC** transitions. On the other hand, the transitions occurring lower than $\approx 31\,000$ cm^{-1} (323 nm) with the maximum at $\approx 26\,500$ cm^{-1} (377 nm, $\epsilon_{max} \approx 130\,00$l/mol cm) result from $\mathbf{S_0}$ to ^{1}**MLCT** (metal-to-ligand-charge transfer) transitions mainly of Ir5d(ppy)π* character. The weakly manifesting shoulders between $\approx 20\,000$ cm^{-1} and $\approx 23\,000$ cm^{-1} correspond to ^{3}**MLCT** states [8,13]. Based on the above assignments, the classification of the absorption spectrum of $Ir(ppy)_2(CO)(Cl)$ (compound **1**) is straightforward. The stronger transitions above $\approx 34\,000$ cm^{-1} (294 nm) correspond to ^{1}**LC** (ppyππ*) states, while the two well recognizable shoulders between $\approx 34\,000$ cm^{-1} (295 nm) and $\approx 26\,000$ cm^{-1} (385 nm) can be assigned to ^{1}**MLCT** states of Ir5d (ppy)π* character. In particular, these $\mathbf{S_0} \rightarrow {}^1$**MLCT** transitions experience relatively large shifts to higher energy (blue shifts) as compared to the corresponding transitions of $Ir(ppy)_3$. Thus in $Ir(ppy)_2(CO)(Cl)$, the transitions $\mathbf{S_0} \rightarrow {}^1$**MLCT** and $\mathbf{S_0} \rightarrow {}^1$**LC** partly overlap. Therefore, the spectrum of $Ir(ppy)_2(CO)(Cl)$ is less well resolved and shows a step-like absorption spectrum (Fig. 1).

The observed blue shifts of the $\mathbf{S_0} \rightarrow {}^1$**MLCT** transitions of $Ir(ppy)_2(CO)(Cl)$ relative to the ones of $Ir(ppy)_3$ are related to the stabilization of the Ir5d(ppy)π orbital (HOMO) as compared to the HOMO of $Ir(ppy)_3$ due to the strong π acceptor ability of the (CO)-ligand and the resulting backbonding effect. Interestingly, also the maxima corresponding to the ^{1}**LC** transitions of $Ir(ppy)_2(CO)(Cl)$ appear to be blue shifted relative to the ones of $Ir(ppy)_3$. However, the 0–0 positions of the lowest energy $\mathbf{S_0} \rightarrow {}^1$**LC** transitions – being coarsely estimated by extrapolation – lie roughly near 32 000 cm^{-1} (313 nm) for both compounds. In Section 4, this aspect is recalled.

Fig. 1 reproduced also the emission spectrum of $Ir(ppy)_2(CO)(Cl)$ measured under ambient conditions in THF. The emissive state is assigned to be dominantly of ^{3}**LC** character with small ^{1}**MLCT** admixtures. The basis of this assignment will be worked out in the subsequent sections.

3.2. Emission spectra – temperature dependence

Fig. 2 shows the 2.2 K (a), 25 K (b), and 300 K (c) emission spectrum of $Ir(ppy)_2(CO)(Cl)$ dissolved in THF under excitation with the 363.8 nm Ar^+-laserline.

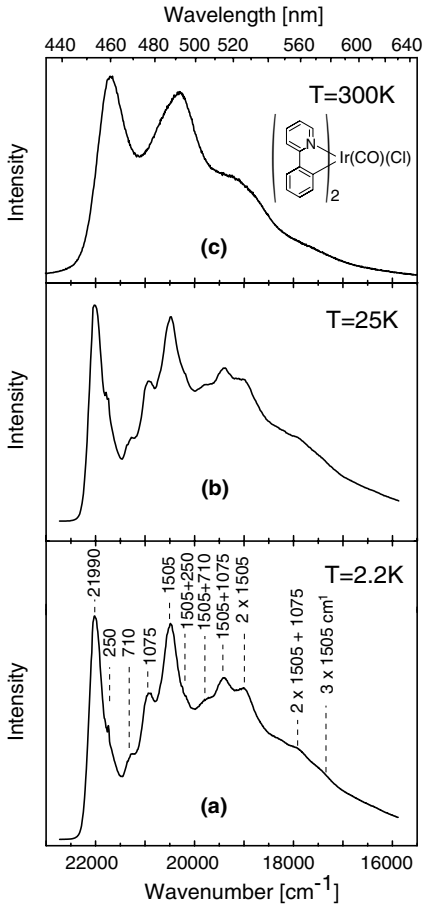

Fig. 2. Emission spectra of $Ir(ppy)_2(CO)(Cl)$ in THF (10^{-5} mol/l) at selected temperatures under cw excitation at 363.8 nm.

The spectrum recorded at 2.2 K is clearly structured. The high energy peak at 21 990 cm^{-1} (455 nm) is assigned to the 0–0 transition (electronic origin) between the $\mathbf{T_1}$ state and the ground state $\mathbf{S_0}$. The peaks of lower energy represent vibrational satellites. Although the spectrum is not well resolved, a number of satellites can clearly be identified. One observes vibrational fundamentals (250, 710, 1075, and 1505 cm^{-1}), combinations (e.g. $1505 + 250$, $1505 + 1075$ cm^{-1}), and a progression (1×1505, 2×1505, and probably 3×1505 cm^{-1}). Corresponding fundamentals of very similar energies have also been observed as satellites in highly resolved emission spectra of $Pt(ppy)_2$, such as 254, 720, 1071, and 1483 cm^{-1} [14]. Beside the distinct inhomogenous broadening effects, the obtainable resolution is also restricted due to the coupling of vibrational satellites to low-energy lattice modes. The emission spectra of $Ir(ppy)_2(CO)(Cl)$ remain nearly unchanged in the temperature range from $T = 2$ K to more than 100 K, apart from a slight smearing out of the vibrational satellite structure. This indicates that no further electronic state contributes to the emission in the corresponding energy range. This behavior is very different from the one found for compounds that are characterized by typical ^{3}**MLCT** states with significant triplet splittings into substates, such as $Ir(ppy)_3$ [8], $Pt(thppy)_2$ (with thpy = 2-(2′-thienyl)pyridine) [15,16] and $[Ru(bpy)_3]^{2+}$ (bpy = 2,2′-bipyridine) [17]. From emission decay dynamics at low temperatures, it can be concluded that the substates **I**, **II**, and **III** of the lowest triplet $\mathbf{T_1}$ of $Ir(ppy)_2(CO)(Cl)$ are split by less than 1 cm^{-1}. All three substates contribute to the emission in the whole temperature range. Further increase of the temperature to 300 K leads to a red shift of the emission by about 300 cm^{-1} and an additional broadening of the spectrum (Fig. 2). The red shift is largely ascribed to the melting of THF at $T = 165$ K [8,18]. Moreover, a decrease of the total emission intensity which is also observed with temperature increase is attributed to an enhanced oxygen quenching in the liquid phase.

3.3. Emission decay times and energy level diagram

Fig. 3 shows emission decay curves of $Ir(ppy)_2(CO)(Cl)$ measured at $T = 1.2$ K and $T = 30$ K. Interest-

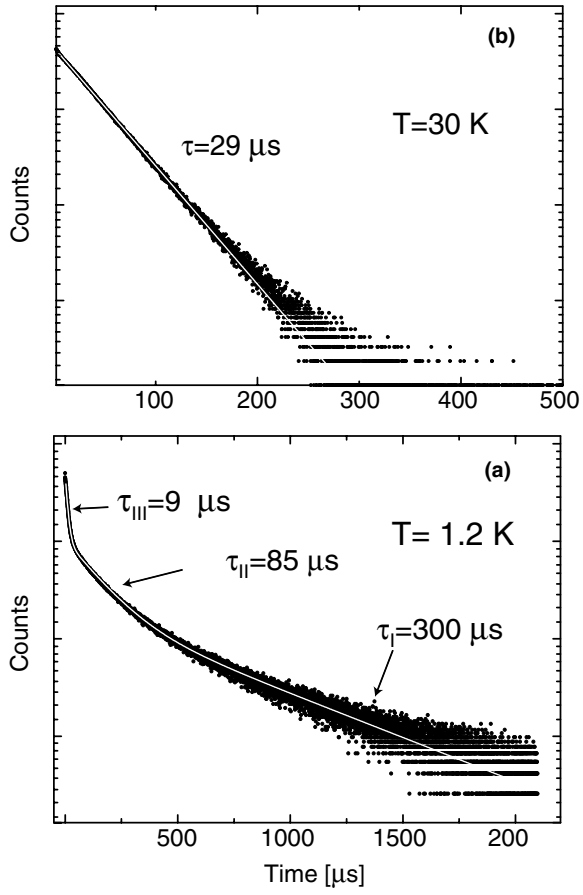

Fig. 3. Emission decay curves (ln scales) of $Ir(ppy)_2(CO)(Cl)$ dissolved in THF ($\approx 10^{-5}$ mol/l) for $T = 1.2$ K (a) and at $T = 30$ K (b), respectively. The decay behavior changes with temperature increase from a triexponential to a monoexponential decay. Excitation: $\lambda_{exc} = 337.1$ nm, pulse width 4 ns. Note the different time scales in (a) and (b).

ingly at 1.2 K, $Ir(ppy)_2(CO)(Cl)$ exhibits a triexponential decay with time constants of $\tau_I = 300$ μs, $\tau_{II} = 85$ μs, and $\tau_{III} = 9$ μs [1]. This behavior can be ascribed to emission decays from three different triplet substates **I**, **II**, and **III** that are independently populated. Importantly, at low temperature, thermal equilibration is extremely slow between electronic states with small energy separations, for example of <1 cm^{-1} (e.g. see [15–17,19,20]). Thus, during the lifetimes of the excited states equilibration is usually not attained and the three triplet substates emit individually [15–17,19–21]. Thermalization between such states is induced by processes of spin–lattice relaxation (SLR). For small energy separations between the triplet substates, for example of the order of 1 cm^{-1} or smaller, the *direct process* of SLR can be neglected, since the corresponding relaxation rate is proportional to the third power of the energy separation. Also the other processes of SLR, *Raman* and *Orbach processes* [16,17,19,21,22], do not contribute at low temperature. However, with temperature increase, both of the latter two processes can become important. For example, it has been proposed for $Pd(thpy)_2$ with a splitting of the $\mathbf{T_1}$ state of less than ≈0.3 cm^{-1} [23,24] that the SLR rate according to the Raman process increases with a T^5 temperature dependence and thus dominates near $T = 5$ K [15]. We suggest that the Raman process is also of importance for $Ir(ppy)_2(CO)(Cl)$. The onset of a faster SLR is reflected in the temperature dependence of the emission decay curves. An increasing SLR rate leads to an increasing deviation from the low temperature decay curve. The three different decay times observed at $T = 1.2$ K approximate each other and finally result in a monoexponential decay curve, when the triplet substates are completely thermalized. Fig. 3 illustrates this behavior by comparing the emission decay curves recorded at 1.2 and 30 K, respectively.

When fast thermalization is attained, the decay dynamics can be described by

$$\frac{dN}{dt} = -k_{therm}N = -\sum_i k_i n_i, \tag{1}$$

wherein n_i denotes the Boltzmann occupation number of state i, k_i the total rate constant for depopulation of state i. N is the total number of occupied excited states, and $k_{therm} = 1/\tau_{therm}$ the rate constant for depopulation of the equilibrated (thermalized) system of excited states or the inverse decay time. When the triplet substates lie close to each other (relative to the thermal energy k_BT), one can apply the high temperature limit of Eq. (1) and one obtains for τ_{therm} by use of the decay times of the three triplet substates [19,22]

$$\tau_{therm} = 3\left(\frac{1}{\tau_I} + \frac{1}{\tau_{II}} + \frac{1}{\tau_{III}}\right)^{-1}. \tag{2}$$

Using the decay times measured at $T = 1.2$ K, one finds a value for the thermalized decay time $\tau_{therm} = (24 \pm 2)$ μs. This average value is close to the measured decay time of (25 ± 1) μs at 130 K. It is remarked that a comparison to the emission decay time at ambient temperature is not reasonable due to additional quenching processes that occur in the liquid phase. Nevertheless, the correspondence described proves that the decay times measured at 1.2 K are the individual radiative decay rates of the three substates **I**, **II** and **III**. The absence of a significant influence of SLR on the decay times at $T = 1.2$ K is a basis for a coarse estimate of an upper limit of the energy separation ΔE between the emitting triplet substates (zero-field splitting, ZFS). At very low temperature, only the *direct* process of SLR can be of importance. The corresponding SLR time depends on the inverse third power of the energy separation. Thus, small energy separations are connected with long SLR times [15–17,19–24]. For example in $Pth(thpy)_2$, the energy separation between the two lowest triplet substates is $\Delta E_{II,I} = 7$ cm^{-1} (obtained from highly resolved spectra). One finds a SLR time of 720 ns at $T = 1.2$ K [15,16,19]. For Pt(thpy)-(CO)(Cl) with a total ZFS of 3.8 cm^{-1}, the SLR relaxation time is as long as 3 μs [16,19]. The shortest decay component found for $Ir(ppy)_2(CO)(Cl)$ is 9 μs. Taking this decay time as an lower limit of the SLR time, it follows that the zero field splitting for $Ir(ppy)_2(CO)(Cl)$ is significantly smaller than the value found for Pt(thpy) (CO)(Cl), if similar electron–phonon coupling conditions are assumed. We expect a separation of the triplet substates of less than 1 cm^{-1} (Fig. 4). For comparison it is mentioned that for $Ir(ppy)_3$ with an energy separation between the two lowest triplet substates of $\Delta E_{II,I} = 11.5$ cm^{-1}, the SLR time is even shorter than 300 ns [8] and thus fits to the tendency described.

3.4. Emission decay after resonant $S_0 \rightarrow T_1$ excitation

In contrast to purely organic molecules, the lowest triplet state of an organo-transition metal compound can often be excited directly from the singlet ground state. This is due to spin–orbit coupling carried by the central metal ion which induces a singlet–triplet mixing. As consequence, the $\mathbf{S_0} \rightarrow \mathbf{T_1}$ transition probabilities and thus the radiative rates increase, while the emission decay times decrease. Hence, a short emission decay time is indicative of a marked transition probability, whereas a long decay time points to a forbidden transition. In this respect, $Ir(ppy)_2(CO)(Cl)$ represents an interesting model system, since the longest and the shortest decay time of the three triplet substates differ by more than a factor of thirty. Thus, it seems to be pos-

[1] The decay times here represent refined values. They slightly deviate from those presented on a recent poster in which we reported $\tau_I = 330$ μs, $\tau_{II} = 100$ μs and $\tau_{III} = 9$ μs.

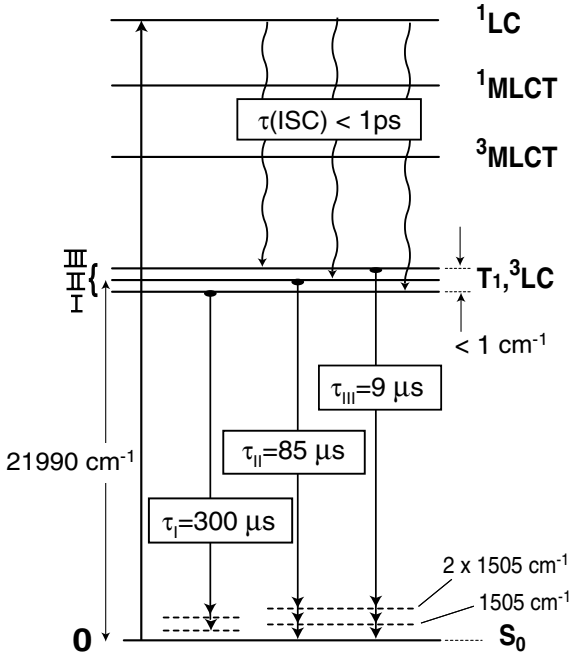

Fig. 4. Energy level diagram for Ir(ppy)$_2$(CO)(Cl) with emphasis on the triplet $\mathbf{T_1}$ substates **I**, **II** and **III**. The energy splitting of ^{3}**LC** of less than 1 cm^{-1} is estimated from the decay behavior (Section 3.3). As an example, a Franck–Condon active (progression forming) mode of 1505 cm^{-1} is depicted. Several higher lying states which are addressed in Section 3.1 are included in the diagram, see also Section 4. τ(ISC): intersystem crossing time (compare [15]). The radiative rate for the 0–0 transition between the substate **I** and the ground state **0** is very often small, hence one finds the long decay time. Often the corresponding radiative deactivation is vibronically induced under action of Herzberg–Teller active vibrational modes. (see also Section 3.4 and [15,17]).

sible to excite and to populate one or two substates *selectively*, while the long-lived one (substate **I**) might not be excitable effectively [2].

Indeed, exactly this behavior is observed (Fig. 5). Pulsed excitation at $\bar{\nu}_{exc} = 21\,846$ cm^{-1} (457.7 nm) corresponding to the inhomogeneously broadened $\mathbf{S_0} \rightarrow \mathbf{T_1}$ 0–0 transition (red flank) leads to a biexponential decay with the components of $\tau_{II} = 85$ μs and $\tau_{III} = 9$ μs at $T = 1.2$ K. This signifies that the substates **II** and **III** are excited selectively. Due to the very slow processes of SLR at $T = 1.2$ K, the spin polarization induced by the excitation pulse is preserved during the emission decay times and one observes just the decay components of these two states, while the long-lived substate **I** is not involved in the emission process. For completeness it is remarked that with temperature increase, the processes of SLR become faster and thus also substate **I** is populated and subsequently emits. This means, with temperature

[2] Often, its emission is only induced by vibronic coupling processes (Herzberg–Teller coupling) with extremely small transition probability of the purely electronic transition [15,17].

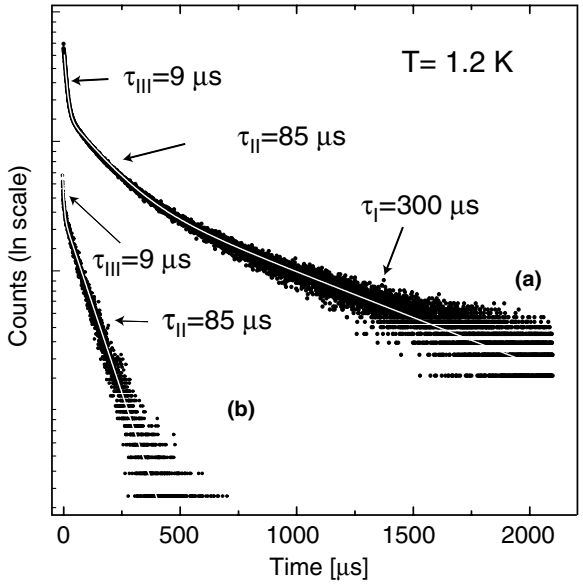

Fig. 5. Emission decay curves (ln scale) of Ir(ppy)$_2$(CO)(Cl) dissolved in THF (≈10^{-5} mol/l) at temperature $T = 1.2$ K. (a) Nonselective excitation at $\bar{\nu}_{exc} = 29\,665$ cm^{-1} (337.1 nm, pulse width 4 ns) leads to three individual decay components. (b) Under selective excitation with a pulse duration of 12 ns at 21 846 cm^{-1} (457.7 nm) only a biexponential decay is observed.

increase a third, long decay component grows in (not shown in Fig. 5).

A similar behavior as found for Ir(ppy)$_2$(CO)(Cl) seems to be characteristic of organo-transition metal compounds with values of ZFS of the order of 1 cm^{-1} or less. For example for Pd(thpy)$_2$ with ZFS of ≈0.3 cm^{-1}, three decay components of 1200, 235, and 130 μs are observed with non-selective excitation, while selective $\mathbf{S_0} \rightarrow \mathbf{T_1}$ excitation at 18 418 cm^{-1} leads only to a biexponential decay with the decay components of 235 and 130 μs. [15] An equivalent situation is found for Ptq$_2$ (with q = qol$^-$ = quinolinole) [25] and [Pt(bpy)$_2$]$^{2+}$ [17,26]. Also for these compounds, the ZFSs are significantly less than 1 cm^{-1}.

In conclusion, the emission decay behavior of Ir(ppy)$_2$(CO)(Cl) at low temperature and under selective $\mathbf{S_0} \rightarrow \mathbf{T_1}$ excitation can only be understood on the basis of a small ZFS (<1 cm^{-1}) of the $\mathbf{T_1}$ state into substates.

4. Assignment and conclusion

We assign the lowest excited triplet state of Ir(ppy)$_2$(CO)(Cl) as ^{3}**LC**(ppyππ*) with small ^{1,3}**MLCT** admixtures. This is mainly based on three spectroscopic features.

4.1. Zero-field splitting

The amount of splitting of the triplet into substates is a consequence of spin–orbit coupling induced by the

d-orbital character in the corresponding triplet wavefunctions. It has been shown in [15,17,19,27] that this value of ZFS can be utilized to classify the orbital character of the triplet state. For example, the large value of ZFS determined for the lowest triplet of $Ir(ppy)_3$ allowed us to assign this state as ^{3}**MLCT**(Ir5d(ppy)π*) state [8]. Further examples are the assignments of the emissive triplets of $[Ru(bpy)_3]^{2+}$ and $[Os(bpy)_3]^{2+}$ for which the ^{3}**MLCT** states are split by about 60 and 210 cm^{-1}, respectively [15,17,19,27]. On the other hand, small ZFSs are characteristic of ligand centered ^{3}**LC** states [15,17,19–21,23,24,26], as has been demonstrated, for example, for $[Rh(bpy)_3]^{3+}$ and $Pd(thpy)_2$ which exhibit values of ZFS of ≈0.1 and ≈0.3 cm^{-1}, respectively [23,24]. For $Ir(ppy)_2(CO)(Cl)$, it could be deduced on the basis of relaxation dynamics that the ZFS splitting is less than 1 cm^{-1}. Thus it follows [15,17,19–21,23,24,26,27] that the lowest triplet represents a ^{3}**LC**(ppyππ*) state.

4.2. Emission decay time

The longest component of emission decay measured at low temperature, for example at $T = 1.2$ K, gives an indication of the allowedness of the corresponding transition. For $Ir(ppy)_2(CO)(Cl)$, the longest decay time amounts to a value of $\tau_I = 300$ μs, while for example for $Ir(ppy)_3$, a significantly shorter decay of $\tau_I = 145$ μs [8] is observed. A similar trend is found, when the averaged decay times of the monoexponential decays measured at higher temperature (e.g. at $T = 130$ K) are compared. Specifically for $Ir(ppy)_2(CO)(Cl)$, we find τ_{therm} (130 K) = 25 μs, whereas for $Ir(ppy)_3$ a value of ≈2 μs was observed [8]. This comparison indicates that the metal participation or **MLCT** admixture in the triplet state of $Ir(ppy)_2(CO)(Cl)$ is significantly smaller than in the emissive triplet of $Ir(ppy)_3$. (For further discussions of such trends compare [15].)

4.3. Temperature dependence and structure of emission spectra

A distinct ZFS and thus well separated triplet substates makes it possible to freeze out the emission from higher lying substates by sufficient temperature reduction. Consequently, an obvious temperature dependence of the emission spectra usually results. Such a behavior was also found for $Ir(ppy)_3$ [8]. On the other hand, for small ZFSs, all three triplet substates emit even at $T = 1.2$ K and temperature increase will not significantly change this situation. Thus, no distinct temperature dependence occurs, as is found for $Ir(ppy)_2(CO)(Cl)$.

Moreover, the structure of the emission spectra is also determined by the strength of metal participation in the emissive state, since the metal character induces the occurrence of additional and overlapping low-energy vibrational satellites of metal–ligand (M–L) vibrational character (⩽600 cm^{-1} from the electronic 0–0 transition) [15]. This property often leads to a smearing-out of the emission spectra. Additionally, inhomogeneity might be more pronounced for ^{3}**MLCT** than for ^{3}**LC** states. This behavior has been observed for the ^{3}**MLCT** emission of $Ir(ppy)_3$ dissolved in THF. The spectrum is broad and largely unstructured, even at 1.2 K [8]. In contrast, the spectrum of $Ir(ppy)_2(CO)(Cl)$ exhibits several resolved vibrational satellites.

In Section 3.1, the lowest singlet state of $Ir(ppy)_2(CO)(Cl)$ has been assigned as ^{1}**MLCT** state, while the preceding discussions clearly show that the emissive triplet is mainly of ^{3}**LC** character. On the other hand for $Ir(ppy)_3$, both the lowest singlet and the emissive triplet are of **MLCT** character (Section 3.1 and [8]). These differences can be rationalized by comparing singlet–triplet splittings, since these depend strongly on the spatial extensions of the involved wavefunctions [15,27]. For example, for a typical **MLCT** excitation of compounds of the third period of transition metal complexes, one finds ^{1}**MLCT**–^{3}**MLCT** splittings of about 3300 cm^{-1} or even smaller, while for typical LC excitations of the type of ligands discussed in this context, the ^{1}**LC**–^{3}**MLCT** splitting amounts to about 9000 cm^{-1} [15,27]. Consequently, it can easily happen that both, ^{1}**MLCT** and ^{3}**MLCT** states, lie *between* the corresponding ^{1}**LC** and ^{3}**LC** states (compare also [6,28,29]). This implies that the sequence of ^{3}**LC** and ^{3}**MLCT** states does not necessarily correlate with the predictions that would result from the redox potentials.

For $Ir(ppy)_2(CO)(Cl)$, the lowest ^{1}**LC** state is estimated to lie roughly near 32 000 cm^{-1} (Section 3.1.) A similar estimate would place the ^{1}**MLCT** state to ≈26 500 cm^{-1}. Indeed, applying the values given for singlet–triplet splittings, one finds that the ^{3}**LC** state may be expected to lie slightly below the ^{3}**MLCT** state. Obviously, on the basis of the rough estimates, a reliable result is not obtainable, but the tendency becomes evident. By detailed experimental studies as carried out in this investigation, one finds that ^{3}**LC** is the emissive state.

For completeness it is remarked that the situation is different for $Ir(ppy)_3$. The lowest ^{1}**MLCT** state (0–0 transition) can be estimated to lie near 23 000 cm^{-1}. With a singlet–triplet splitting of 3300 cm^{-1}, one would expect to find the corresponding ^{3}**MLCT** state near to 19 700 cm^{-1}. A corresponding estimate would place the ^{3}**LC** state to a significantly higher energy, namely to about 23 000 cm^{-1}. Experimentally, for $Ir(ppy)_3$ it is found that the emissive state is of ^{3}**MLCT** character and it lies near 20 500 cm^{-1} [8]. Consequently, the assignment of the type of the emissive triplet state simply by rough estimates based on absorption spectra without applying detailed low-temperature investigations is much more reliable for $Ir(ppy)_3$ than for $Ir(ppy)_2(CO)(Cl)$.

In conclusion, the discussion presented shows that the character of the emitting triplet state, either **^{3}LC** or **^{3}MLCT**, depends on the individual ligands that coordinate the Ir(III) central metal. Both states can have energy separations only of the order of a thousand cm^{-1}. But their emission properties are distinctly different (emission color, decay time, quantum yield, etc.) [27]. Slight shifts of these states relative to each other have drastic photophysical consequences. Therefore, it seems to be attractive to exploit this behavior for a controlled development, for example, of new OLED materials.

Acknowledgements

We thank the *Bundesministerium für Bildung und Forschung (BMBF)* for providing funding.

References

[1] J. Li, P.I. Djurovich, B.D. Alleyne, I. Tsyba, N.N. Ho, R. Bau, M.E. Thompson, Polyhedron 23 (2004) 419.
[2] R.J. Holmes, B.W. D'Andrade, S.R. Forrest, X. Ren, J. Li, M.E. Thompson, Appl. Phys. Lett. 83 (2003) 3818.
[3] X.H. Yang, D. Neher, Appl. Phys. Lett. 84 (2004) 2476.
[4] I.R. Laskar, T.-M. Chen, Chem. Mater. 16 (2004) 111.
[5] S. Lamansky, P.I. Djurovich, F. Abdel-Razzaq, S. Garon, D.L. Murphy, M.E. Thompson, J. Appl. Phys. 92 (2002) 1570.
[6] M.G. Colombo, H.U. Güdel, Inorg. Chem. 32 (1993) 3081.
[7] K.A. King, P.J. Spellane, R.J. Watts, J. Am. Chem. Soc. 107 (1985) 1431.
[8] W.J. Finkenzeller, H. Yersin, Chem. Phys. Lett. 377 (2003) 299.
[9] P.J. Hay, J. Phys. Chem. A 106 (2002) 1634.
[10] S. Sprouse, K.A. King, P.J. Spellane, R.J. Watts, J. Am. Chem. Soc. 106 (1984) 6647.
[11] E. Gallhuber, G. Hensler, H. Yersin, J. Am. Chem. Soc. 109 (1987) 4818.
[12] A.B. Tamayo, B.D. Alleyne, P.I. Djurovich, S. Lamansky, I. Tsyba, N. Ho, R. Bau, M. Thompson, J. Am. Chem. Soc. 125 (2003) 7377.
[13] W.J. Finkenzeller, P. Stößel, M.V. Kulikova, H. Yersin, Proc. SPIE 5214 (2003) 356.
[14] H. Yersin, Top. Curr. Chem. 241 (2004) 1.
[15] H. Yersin, D. Donges, Top. Curr. Chem. 214 (2001) 81.
[16] J. Strasser, H.H.H. Homeier, H. Yersin, Chem. Phys. 255 (2000) 301.
[17] H. Yersin, W. Humbs, J. Strasser, Top. Curr. Chem. 191 (1997) 153.
[18] P. Chen, T.J. Meyer, Chem. Rev. 98 (1998) 1439.
[19] H. Yersin, J. Strasser, Coord. Chem. Rev. 208 (2000) 331.
[20] J. Strasser, D. Donges, W. Humbs, M.V. Kulikova, K.P. Balashev, H. Yersin, J. Lumin. 76–77 (1998) 611.
[21] J. Schmidt, J. Strasser, H. Yersin, Inorg. Chem. 36 (1997) 3957.
[22] D.S. Tinti, M. El-Sayed, J. Chem. Phys. 54 (1971) 2529.
[23] M. Glasbeek, R. Sitters, E. van Veldhofen, A. von Zelewsky, W. Humbs, H. Yersin, Inorg. Chem. 37 (1998) 5159.
[24] M. Glasbeek, Top. Curr. Chem. 213 (2001) 95.
[25] D. Donges, J.K. Nagle, H. Yersin, Inorg. Chem. 36 (1997) 3040.
[26] W. Humbs, H. Yersin, Inorg. Chim. Acta 265 (1997) 139.
[27] H. Yersin, Top. Curr. Chem. 241, 2004 (in press).
[28] M.G. Colombo, A. Hauser, H.U. Güdel, Inorg. Chem. 32 (1993) 3088.
[29] M.G. Colombo, A. Hauser, H.U. Güdel, Top. Curr. Chem. 171 (1994) 143.